Sphingopeptides: dihydrosphingosine-based fusion inhibitors against wild-type and enfuvirtide-resistant HIV-1

Avraham Ashkenazi,* Mathias Viard,[†,‡] Linor Unger,* Robert Blumenthal,[†] and Yechiel Shai*,[1]

*Department of Biological Chemistry, The Weizmann Institute of Science, Rehovot, Israel; [†]Nanobiology Program, Center of Cancer Research, Frederick National Laboratory, National Cancer Institute, Frederick, Maryland, USA; and [‡]Basic Science Program, SAIC-Frederick, Inc., Center for Cancer Research Nanobiology Program, Frederick National Laboratory, Frederick, Maryland, USA

ABSTRACT **Understanding the structural organization of lipids in the cell and viral membranes is essential for elucidating mechanisms of viral fusion that lead to entry of enveloped viruses into their host cells. The HIV lipidome shows a remarkable enrichment in dihydrosphingomyelin, an unusual sphingolipid formed by a dihydrosphingosine backbone. Here we investigated the ability of dihydrosphingosine to incorporate into the site of membrane fusion mediated by the HIV envelope (Env) protein. Dihydrosphingosine as well as cholesterol, fatty acid, and tocopherol was conjugated to highly conserved, short HIV-1 Env-derived peptides with no antiviral activity otherwise. We showed that dihydrosphingosine exclusively endowed nanomolar antiviral activity to the peptides (IC_{50} as low as 120 nM) in HIV-1 infection on TZM-bl cells and on Jurkat T cells, as well as in the cell-cell fusion assay. These sphingopeptides were active against enfuvirtide-resistant and wild-type CXCR4 and CCR5 tropic HIV strains. The anti-HIV activity was determined by both the peptides and their dihydrosphingosine conjugate. Moreover, their mode of action involved accumulation in the cells and viruses and binding to membranes enriched in sphingomyelin and cholesterol. The data suggest that sphingopeptides are recruited to the HIV membrane fusion site and provide a general concept in developing inhibitors of sphingolipid-mediated biological systems.—Ashkenazi, A., Viard, M., Unger, L., Blumenthal, R., Shai, Y. Sphingopeptides: dihydrosphingosine-based fusion inhibitors against wild-type and enfuvirtide-resistant HIV-1. *FASEB J.* 26, 4628–4636 (2012). www.fasebj.org**

Key Words: viral envelope protein · sphingolipids

THE FIRST STEP IN THE life cycle of enveloped viruses is entry into their host cells by membrane fusion (1). To mediate fusion, the viral envelope (Env) protein needs to assist in overcoming the energy barriers to fusion imposed by its surrounding lipids (2). Emerging studies on HIV and other viruses, such as influenza, West Nile, and murine coronavirus, suggest membrane-ordered domains as a lipid platform for virus release and entry (3–9). This results in viral envelopes with elevated levels of ordered lipid domains (10). Ordered lipid domains are assemblies in cell membranes that are enriched in cholesterol and sphingolipids (11). The formation of these domains and the partitioning of proteins and lipids into them are dynamic processes (12). Therefore, it is of great importance to identify lipids that can be incorporated into the fusion site during the dynamics of the membrane fusion events.

The HIV Env is composed of 2 noncovalently associated subunits: the gp120 subunit enables binding of cell receptors and coreceptors, whereas the gp41 transmembrane subunit mediates the physical membrane fusion reaction (13–15). Binding of gp120 to CD4 and a coreceptor involves conformational changes in both gp120 and gp41, resulting in gp41 prehairpin conformation (14, 16, 17). This conformation is sensitive to gp41-derived peptide fusion inhibitors that capture it in an intermediate state (18–22). As a result, the folding of the protein into the hairpin conformation is prevented, leading to inhibition of viral fusion. The hairpin conformation (23) comprises a trimeric central coiled-coil that is created by 3 N-terminal heptad repeat (NHR) regions, into which three C-terminal heptad repeat (CHR) regions are packed in an antiparallel manner (24, 25). The structure is usually referred to as the "6-helix bundle" or "core" structure, which is required for complete membrane fusion. Similar

Abbreviations: DCM, dichloromethane; DEAE, diethylaminoethyl; DIEA, *N,N*-diisopropylethylamine; DMF, dimethylformamide; Env, envelope; LUV, large unilamellar vesicle; NBD, 4-fluoro-7-nitrobenzofurazan; NHR, N-terminal heptad repeat; CHR, C-terminal heptad repeat; TFA, trifluoroacetic acid; VSV-G, vesicular stomatitis virus G

[1] Correspondence: Department of Biological Chemistry, The Weizmann Institute of Science, Rehovot, 76100 Israel. E-mail: yechiel.shai@weizmann.ac.il

doi: 10.1096/fj.12-215111

This article includes supplemental data. Please visit *http://www.fasebj.org* to obtain this information.

0892-6638/12/0026-4628 © FASEB

bundles are created in other viral fusion proteins and in intracellular vesicle fusion by soluble *N*-ethylmaleimide-sensitive factor accessory protein receptor proteins, demonstrating a common mechanism in diverse systems (26).

The HIV lipidome shows a remarkable enrichment in dihydrosphingomyelin (10). This is an unusual sphingolipid in which the backbone is formed by dihydrosphingosine (sphinganine; refs. 27, 28). In this study, we investigated the ability of sphinganine to incorporate into the site of the HIV Env-mediated fusion reaction. For this purpose, sphinganine and other lipids from different classes were conjugated to highly conserved short fragments from the Env core that could capture the Env in its intermediate state and inhibit fusion when they are in proximity (**Fig. 1**). We hypothesized that by minimizing the affinity of the peptides to the viral fusion site (using short fragments from the core); we would mainly identify the contribution of the conjugated lipid moiety to antiviral activity. We showed that sphinganine endowed significant antiviral activity to otherwise poorly and nonactive, short C and N peptides derived from the core in enfuvirtide-resistant and wild-type HIV-1. We address its plausible mode of action in the context of the lipid-protein rearrangements underlying virus-mediated cell fusion.

MATERIALS AND METHODS

Peptide synthesis, lipid moiety conjugation, and fluorescent labeling

Peptides were synthesized on Rink amide MBHA resin (Novabiochem AG, Laufelfingen, Switzerland) by using the F-moc strategy as described previously (29). Several peptides contain a lysine residue at their C terminus with an 3-(4,5-dimethyl-2-thizolyl)-2,5-diphenyl-2*H*-tetrazolium bromide side chain protecting group (Novabiochem) that requires a special deprotection step under mild acidic conditions [two 1-min washes of 5% trifluoroacetic acid (TFA) in dichloromethane (DCM) and 30 min of 1% TFA in DCM]. This enables the conjugation of a lipid moiety or a fluorescent probe to the C terminus. Conjugation of hexadecanoic (palmitic) acid (C16) or α-tocopherol succinate (Sigma-Aldrich, Rehovot, Israel) to the N terminus of selected peptides was performed using standard F-moc chemistry. Conjugation of cholesterol to the N terminus of a peptide was performed by adding 10 equivalents of cholesteryl chloroformate (Alfa Aesar, Ward Hill, MA, USA) dissolved in DCM, together with 3 equivalents of triethylamine to the peptide resin. Conjugation of D-erythro-dihydrosphingosine (D-erythro-sphinganine; Matreya, LCC, State College, PA, USA) to the N or C terminus of a peptide was performed as follows: first, 10 equivalents of *N,N′*-disuccinimidyl carbonate (Chem-Impex International, Wood Dale, IL, USA) and 20 equivalents of *N,N*-diisopropylethylamine (DIEA) were added to the resin for 2 h in dimethylformamide (DMF). Then, 2 equivalents of sphinganine and 2 equivalents of DIEA were added for overnight incubation in DMF anhydrous. Addition of NBD-F, a fluoride [4-fluoro-7-nitrobenzofurazan (NBD)] fluorescent probe (Biotium, Hayward, CA, USA), to the N or C terminus of selected peptides was performed in DMF for 1 h. All peptides were cleaved from the resin by a TFA/double-distilled water/*N*-tris(hydroxymethyl) methyl-2-aminoethanesulfonic acid (93.1:4.9:2, v/v) mixture and purified by reverse-phase HPLC to >95% homogeneity. The molecular weight of the peptides was confirmed by platform electrospray mass spectrometry. For hydrophobicity tests, the peptides were eluted with a flow rate of 0.6 ml/min using a 2-step linear gradient from CH_3CN/H_2O (20:80, v/v) to CH_3CN/H_2O (95:5, v/v) in 30 min and from CH_3CN/H_2O (95:5, v/v) to CH_3CN/H_2O (95:5 in 10 min, v/v) on a Nucleosil analytical C2 column (7-μm particle size, pore size 100 Å; Macherey-Nagel, Düren, Germany).

HXB2 virus infectivity assay

A stock of fully infectious HIV-1 HXB2 concentrated virus was a kind gift from the AIDS Vaccine Program (SAIC-Frederick,

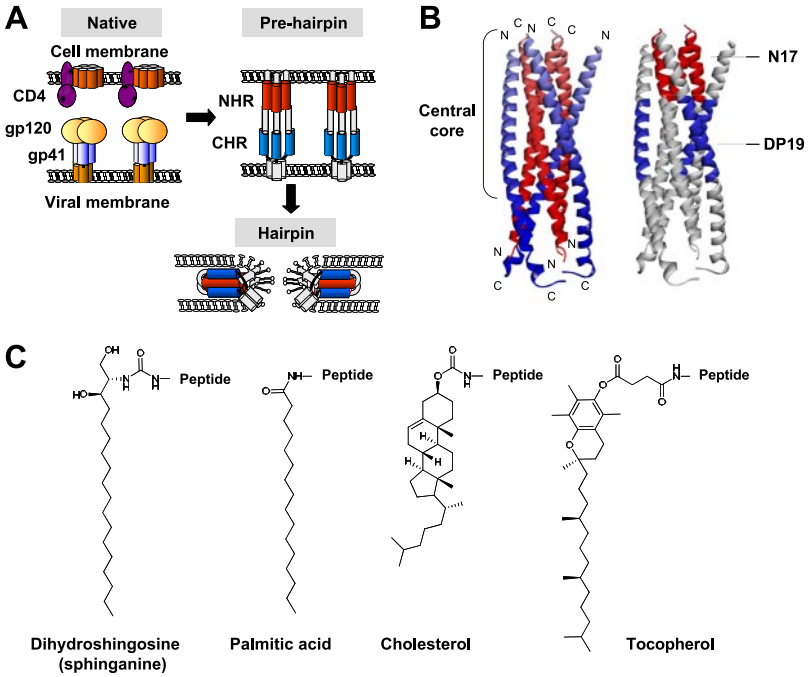

Figure 1. Model for HIV membrane fusion and the structure of lipids investigated in this study. *A*) HIV gp41 transmembrane protein has at least 3 major conformations during membrane fusion: the native nonfusogenic conformation, the prehairpin conformation, and the hairpin conformation. *B*) Side view of the recently determined hairpin structure of gp41 (Protein Data Bank identification number 2X7R; ref. 56). The trimeric inner coiled-coil of the N helices is shown in red; the 3 packing C helices are in blue. C, carboxyl terminus; N, amino terminus. Investigated short domains within the central core of the protein are indicated: the 17-mer conserved pocket sequence, termed N17; and the 19-mer N-helix binding sequence, termed DP19. *C*) Chemical structures of the hydrophobic conjugates investigated: the cellular moieties consisted of dihydrosphingosine (sphinganine), palmitic acid, and cholesterol; the noncellular moiety consisted of tocopherol.

Inc., National Cancer Institute–Frederick, Frederick, MD, USA). The infectivity of HIV-1 HXB2 was determined using the TZM-bl cell line as a reporter. Cells were added (2×10^4 cells/well) to a 96-well clear-bottomed microtiter plate with 10% serum-supplemented DMEM. Plates were incubated at 37°C for 18-24 h to allow the cells to adhere. The mediam was then aspirated from each well and replaced with serum-free DMEM containing 40 μg/ml diethylaminoethyl (DEAE)-dextran. Stock dilutions of each peptide were prepared in DMSO so that each final concentration was achieved with 1% dilution. On addition of the peptides, the virus was added to the cells diluted in serum-free DMEM containing 40 μg/ml DEAE-dextran. The plate was then incubated at 37°C for 18 h to allow the infection to occur. Luciferase activity was analyzed using the Steady-Glo Luciferase Assay Kit (Promega, Madison, WI, USA). Sometimes cell-washing experiments were performed, as follows: peptides were preincubated with TZM-bl cells at 37°C for 1 h, followed by 3 washes with culture medium to remove unbound peptides and the addition of HXB2 viruses to start the infection. After 18 h, the antiviral activities of the remaining peptides that survive the washing were determined by measuring luciferase activity as described previously. For the virus treatment experiment, the virus was diluted in 100 μl of serum-free DMEM, and sphingopeptides were added in DMSO to a final concentration of 2 μM. After a 10-min incubation at room temperature, 400 μl of PBS was added. The sample was then centrifuged using Amicon centrifugal filters (EMD Millipore, Billerica, MA, USA) with a 30-kDa cutoff for 15 min at 10,000 *g*. The viruses were recovered (40 μl), and their infectivity was tested using the TZM-bl cell line as described above.

Fitting of the data points was performed according to Eq. 1, derived from the Hill equation, as described previously (30):

$$Y(x) = Bx\left(\frac{A^C}{X^C + A^C}\right) \quad (1)$$

In brief, in this equation, B is the maximum value; therefore, it equals 100% fusion, A is the value of an inhibitory concentration at 50% viral infectivity (IC_{50}), and c represents the Hill coefficient. For the fitting, we uploaded the X and Y values of the data into a nonlinear least-squares regression (curve fitter) program that provided the IC_{50} value (parameter A).

Infection with pseudotyped viruses

Cotransfection of 293T cells with the pNLLuc plasmid and HIV LAI Env, vesicular stomatitis virus G (VSV-G) Env [obtained from the U.S. National Institutes of Health (NIH) AIDS Research and Reference Reagent Program], and HIV AD8 Env (a gift from Dr. Eric Freed, National Cancer Institute, Bethesda, MD, USA) plasmids was performed. After 48 h of transfection, the viral supernatant was harvested and titrated with the TZM-bl cells. The pseudoviruses thus generated have the same core and differ only by the fusion protein present on their surface. Infectivity assays were performed as described for the HXB2 assay. To assess viral infection with Jurkat clone E6-1 T cells, LAI-pseudotyped viruses were used. The Jurkat cells were used at 1.5×10^4 cells/well, and the infection was performed for 3 d.

Enfuvirtide-resistant virus infection

Virus stocks of the wild-type LAI and V38E mutant were prepared with the use of infectious molecular clones as described previously (31). Molecular clones of HIV-1 LAI and NL4-3 were obtained from the NIH AIDS Research and Reference Reagent Program. *Eco*RI-*Xho*I fragments from the LAI molecular clone were cloned into pcDNA3.1 expression vector (Invitrogen, Carlsbad, CA, USA), making the wild-type LAI Env construct. The fragment contains open reading frames of *env*, *tat*, and *rev* genes. Point mutation (V38E) was introduced in the wild-type Env construct using the QuikChange Site-Directed Mutagenesis Kit (Stratagene, La Jolla, CA, USA). The mutant was numbered based on the Env sequence of the HXB2 reference strain. The mutant Env region was also introduced into the NL4-3 molecular clone using the *Eco*RI-*Xho*I fragments to generate infectious molecular clones containing mutant LAI Env. Next, 293T cells were transfected with the infectious molecular clones. The virus supernatant was collected 48 h post-transfection, cleared of cellular debris by centrifugation, portioned into aliquots, and stored at −70°C. Infection with those viruses was performed as described previously for the HXB2 virus.

Cell-cell fusion assay

Effector cells were the Env-expressing cells, HL2-3, a HeLa-derived cell line, which constitutively expresses the HXB2 strain of the HIV-1 Env glycoprotein along the Tat protein, and as target cells, TZM-bl cells were used. The fusion of HL2-3 cells with TZM-bl cells was assessed through luciferase expression. The TZM-bl cells were seeded at 2×10^4 cells/well overnight in a 96-well plates. The medium was then aspirated from each well and replaced with serum-free DMEM containing 40 μg/ml DEAE-dextran. Stock dilutions of each peptide were prepared in DMSO so that each final concentration was achieved with 1% dilution. On addition of the peptides, the HL2-3 cells were added to the TZM-bl cells in serum-free DMEM containing 40 μg/ml DEAE-dextran at a 1:1 cell ratio. The cells were cocultured at 37°C for 6 h to allow the fusion to occur. Luciferase activity was analyzed using the Steady-Glo Luciferase Assay Kit.

Preparation of lipid vesicles

Large unilamellar vesicles (LUVs) were prepared as described previously (32) from egg phosphatidylcholine, cholesterol, and egg yolk sphingomyelin (Sigma-Aldrich). A dried film of lipids containing a total of 2 mg of phosphatidylcholine/sphingomyelin/cholesterol (1:1:1) or 2 mg of phosphatidylcholine/cholesterol (9:1) was suspended in PBS and vortexed for 1.5 min. The lipid suspension underwent 5 cycles of freezing-thawing and then extrusion through polycarbonate membranes with 1- and 0.1-μm diameter pores for 25 times.

Peptide binding to LUVs

The degree of peptide association with lipid vesicles was measured by addition of lipid vesicles to 0.1 μM fluorescent NBD-labeled peptides at room temperature, as described previously (33). The fluorescence intensity was measured as a function of the lipid/peptide molar ratio, with excitation set at 467 nm (10-nm slit) and emission set at 530 nm (10-nm slit). To determine the extent of the contribution of the lipid to any given signal, the readings after the addition of lipid vesicles were subtracted as background from the recorded fluorescence intensity. The affinity constants were then determined by a steady-state affinity model using nonlinear least squares. The nonlinear least squares fitting was done using Eq. 2:

$$Y(x) = \frac{K_a \times X \times F_{\max}}{1 + K_a \times X} \quad (2)$$

where X is the lipid concentration, $Y(x)$ is the fluorescence emission, $F_{\max}$ is the maximal difference in the emission of

TABLE 1. *Antiviral activity and biochemical properties of N17 peptides and their different lipid conjugates*

Peptide	IC_{50} (μM)[a]	Hydrophobicity (min)[b]	Helicity (%)[c]
N17	>4	18.2	20
Palmitic acid-N17	>4	26.7	<10
Cholesterol-N17	>4	28.9	<10
Tocopherol-N17	>4	28.9	<10
Sphinganine-N17	0.121 ± 0.036	27.2	<10

[a]Inhibition of viral infection. TZM-bl cells were infected with fully infectious HXB2 HIV-1 in the presence of different compounds. IC_{50} for each compound was calculated as described in Materials and Methods. Results are means ± SD); $n = 3$. [b]Hydrophobicity was analyzed by RP-HPLC. Retention time of each compound is presented. [c]Percentage of α-helical structure was determined as described in Materials and Methods.

NBD-labeled peptide before and after the addition of lipids (it represents the maximum peptide bound to lipid), and K_a is the affinity constant.

Determination of secondary structures

Circular dichroism measurements were performed by using a spectropolarimeter (Applied Photophysics, Leatherhead, UK). The spectra were scanned using a thermostatic quartz cuvette with a pathlength of 1 mm. Wavelength scans were performed at 25°C; the average recording time was 15 s, in 1-nm steps, in the wavelength range of 190-260 nm. Each peptide concentration was 10 μM in HEPES buffer (5 mM, pH 7.4). Fractional helicities were calculated as described previously (34).

RESULTS

Sphinganine exclusively endows antiviral activity to a nonactive short conserved gp41 N peptide

The 17-mer sequence, termed the pocket, is a conserved domain within the HIV-1 gp41 protein core. This is a deep cavity on the surface of the grooves of the NHR trimer that is important for stabilizing the trimer; it interacts with the CHR to maintain the stability of the gp41 core (35, 36) However, a synthetic N peptide derived from the pocket domain (termed N17) was not active in inhibiting viral infectivity up to 4 μM, the maximal concentration tested (**Table 1**). We conjugated to N17 the following hydrophobic moieties (Fig. 1*B*, *C*): dihydrosphingosine (sphinganine), which forms the backbone of dihydrosphingomyelin (27, 28); cholesterol; and palmitic acid, which is a building block in many lipids, including phospholipids. For a comparison, we also conjugated to N17 tocopherol, a hydrophobic noncellular compound. The hybrid compounds were tested for their ability to inhibit viral infectivity. Notably, the inhibitory activity of N17 depends on the nature of the lipid moiety (Table 1 and **Fig. 2**). Sphinganine was the most prominent one and potentiated the antiviral activity of N17 into the nanomolar concentration range. This exclusive inhibitory activity of sphinganine-based peptides (sphingopeptides) was further observed in a wider spectrum of viral entry systems, consisting of different HIV strains (wild-type HXB2 and LAI) and different target cells (TZM-bl reporter cells and Jurkat T cells), as well as in cell-cell fusion assay (Fig. 2).

Increased antiviral activity of short peptides is sometimes attributed to increased hydrophobicity (30, 37) or increased α-helical content of the compound *via* conjugation to a specific moiety (38). Therefore, we checked the apparent hydrophobicity of N17 and its lipid conjugates (Table 1). The most hydrophobic compounds were the tocopherol and cholesterol conjugates. Sphinganine and palmitic acid conjugates exhibited similar medium hydrophobicity, and N17 alone was the least hydrophobic. Clearly, there was no correlation between the extent of hydrophobicity and antiviral activity in this case. In addition, there was no increase in the α-helical content of N17 on conjugation (Table 1).

Anti-HIV activity of sphingopeptides is determined by both the peptides and their lipid moiety

We further investigated the interplay between sphinganine and its conjugated peptide in inhibiting viral infectivity. Viruses were constructed to have the same HIV core with three different Envs: LAI (CXCR4 tropic), AD8 (CCR5 tropic), and VSV-G. The three constructed viruses

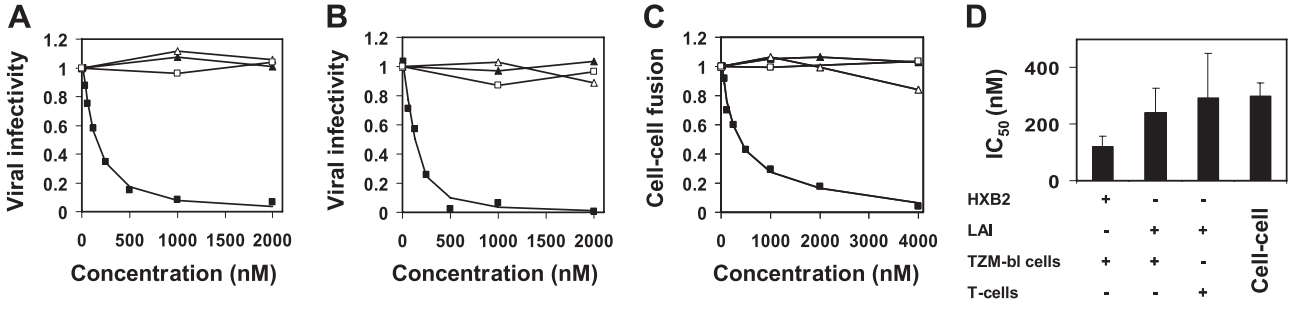

Figure 2. Sphinganine exclusively endows antiviral activity to a short conserved gp41 N peptide in different HIV entry assays. Influence of sphinganine-N17 (■), palmitic acid-N17 (△), cholesterol-N17 (▲), and tocopherol-N17 (□) on HIV entry. *A*) TZM-bl cells that were infected with the wild-type fully infectious HXB2 strain. *B*) Jurkat T cells that were infected with a pseudotyped LAI strain. *C*) TZM-bl target cells that were fused to HIV Env-expressing effector cells. A representative viral infectivity curve is presented. *D*) IC_{50} of sphinganine-N17 in different viral entry systems. Results represent means ± SD (n=3).

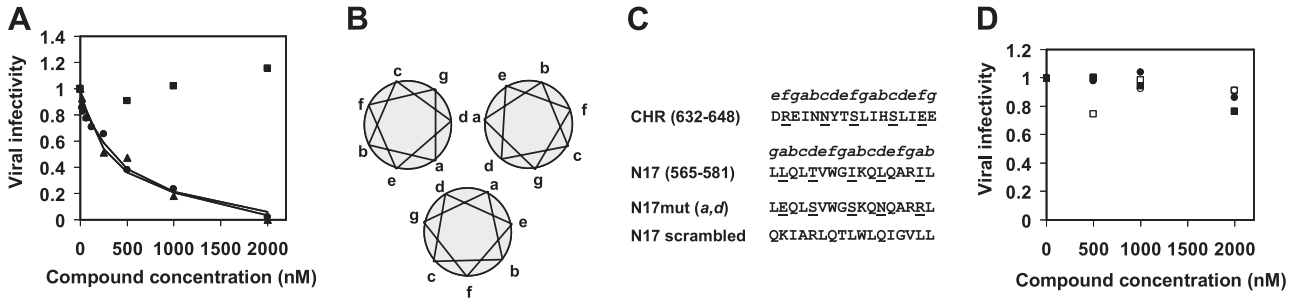

Figure 3. Anti-HIV activity of sphingopeptides is determined by both the peptides and their lipid moiety. *A*) Viruses were constructed to have the same HIV core with 3 different Envs: LAI (CXCR4 tropic), AD8 (CCR5 tropic), and VSV-G. The 3 constructed viruses were allowed to infect TZM-bl cells in the presence of increasing concentrations of sphinganine-N17. Representative viral infection inhibitory curves are presented ($n=2$) for LAI (▲), AD8 (●), and VSV-G (■). Corresponding IC_{50} values of LAI and AD8 were 312 ± 83 and 403 ± 70 nM. *B*) Helical wheel representation demonstrates the interaction between the NHR regions of HIV gp41 in the core structure of the hairpin conformation, as observed in the crystal structures. Intermolecular association between the N helices occurs between positions *a* and *d* of the helical wheel. *C*) Mutational analysis of N17 interactions. In the N17mut(*a,d*) mutant (39), the residues at positions *a* and *d* of N17 were replaced by residues at positions *f* and *c*, respectively, of the CHR (residues are underscored). Residue numbers correspond to the HXB2 gp160 variant. In the scrambled N17 mutant, the residues of N17 were randomized. *D*) Sphingopeptides with mutated peptides, unable to self-interact or scrambled, lose their antiviral activity. TZM-bl cells were infected with fully infectious HXB2 HIV-1 in the presence of increasing concentrations of N17mut(*a,d*) (●), sphinganine-N17mut(*a,d*) (○), scrambled N17 (■), and sphinganine-scrambled N17 (□).

were allowed to infect TZM-bl cells in the presence of increasing concentrations of sphingopeptides (**Fig. 3*A***). Antiviral activity was observed for LAI and AD8 but not for VSV-G.

The importance of peptide interactions to the overall activity of the molecules was examined using sequence mutagenesis. Mutated sphingopeptides were prepared by replacing N17 peptides residues in positions *a* and *d* of the helical wheel, termed N17m(*a,d*), thus knocking out their ability to self-assemble (Fig. 3*B*, *C*). The rationale followed the report by Bewley *et al.* (39) for N36 peptides, in which these mutations completely abrogated N-peptide antiviral activity. Alternatively, we randomly reorganized the N17 sequence to give scrambled peptides (Fig. 3*C*). None of the mutant N17 peptides or their sphinganine conjugates showed antiviral activity (Fig. 3*D*). In addition, a 17-mer N peptide was synthesized from the same region as N17 but shifted in its sequence from the gp41 pocket (the peptide termed ShN17; **Fig. 4*A***). Sphingopeptides comprising the ShN17 sequence exhibited antiviral activity that was 7.3-fold lower than those with the pocket

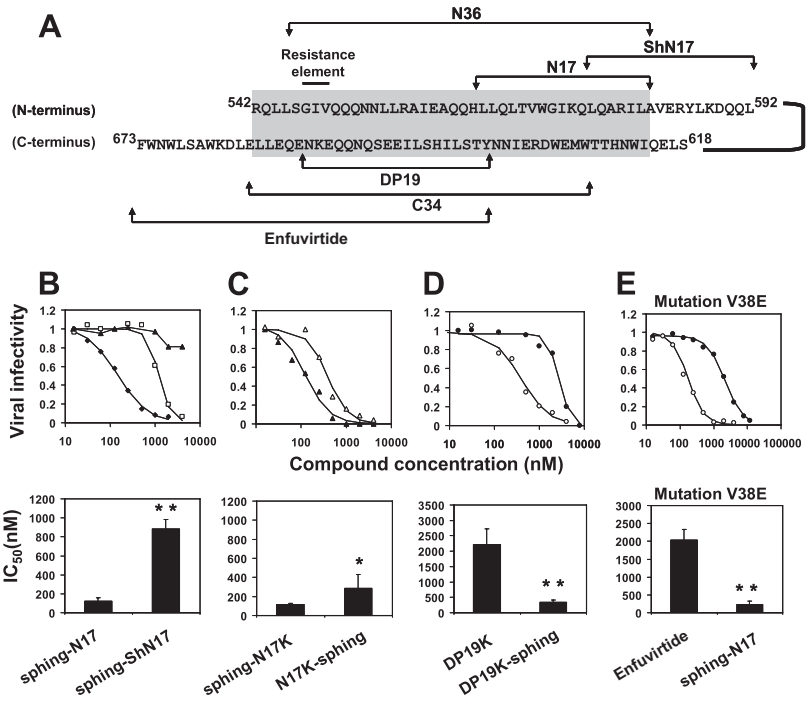

Figure 4. Sphinganine potentiates the activity of N and C peptides in wild-type and enfuvirtide-resistant viruses. *A*) Designation and location of the peptides within the gp41 core. The complex between N36 from the N helix and C34 from the C helix resembles the central core and is highlighted. The short domains N17 and DP19 are located within the central core, whereas the ShN17 extends from the core. Residue numbers correspond to the HXB2 gp160 variant. *B–D*) Viral infection inhibitory curves of the compounds and their corresponding IC_{50} values. TZM-bl cells were infected with fully infectious HXB2 HIV-1 in the presence of increased concentrations of the indicated compounds. *B*) Sphinganine (▲), sphinganine-N17 (sphing-N17; ♦), and sphinganine-ShN17 (sphing-ShN17; □). *C*) N-terminal conjugated N17K (sphing-N17K; ▲) or C-terminal conjugated N17K (N17K-sphing; △). *D*) DP19K alone (●) and DP19K-sphinganine (DP19K-sphing; ○). *E*) Cells were infected with fully infectious enfuvirtide-resistant LAI strain with an escape mutation in the gp41 core (V38E). Viral infection inhibitory curve of the drug enfuvirtide (●) and sphing-N17 (○) as well as their corresponding IC_{50} values are presented. IC_{50} values are presented as means ± SD, $n \geq 3$. $^*P < 0.05$, $^{**}P < 0.02$.

sequence (Fig. 4*B*). The addition of sphinganine alone, up to 1 μM (a concentration at which sphinganine-N17 completely blocks fusion), did not affect viral infectivity (Fig. 4*B*).

Sphinganine potentiates the activity of short N and C peptides in wild-type and enfuvirtide-resistant virus

Changing the orientation of sphinganine toward N17 was achieved by addition of lysine to its C terminus, enabling C-terminal lipid conjugation. The addition of the lysine did not alter the antiviral activity of the compound according to its inhibitory concentration at 50% infectivity (IC_{50}) of 121 ± 36 and 116 nM ± 12 nM to sphinganine-N17 and sphinganine-N17K, respectively (Fig. 4*B*, *C*). The inhibitory potentiation of sphinganine was still powerful *via* C-terminal conjugation, exhibiting an IC_{50} value of 287 ± 143 nM to N17K-sphinganine (Fig. 4*C*). We then investigated whether the ability of sphinganine to potentiate the activity of short N peptides could be exploited to other peptides from the gp41 core. Therefore, a short 19-mer C peptide from the CHR, termed DP19, was synthesized (Figs. 1*B* and 4*A*). DP19K-sphinganine was significantly more potent than DP19K, exhibiting an IC_{50} value of 350 ± 60 nM (Fig. 4*D*). Accordingly, this amplification of fusion inhibition is not restricted only to N peptides. It can be implemented in other short fragments from different regions within the gp41 core.

The GIV sequence within the NHR of gp41 (Fig. 4*A*) is well established as a site for escape mutations of the virus against the fusion inhibitor drug, enfuvirtide, which leads to viral resistance (40). We introduced to the HIV construct a mutation in the GIV sequence (V38E) that considerably weakened the antiviral activity of enfuvirtide, whereas sphinganine-N17 preserved its potent antiviral activity (Fig. 4*E*).

Sphingopeptides strongly bind and accumulate in the viral membrane and in the cell membrane

The ability of sphingopeptides to bind and accumulate in the cell membrane was examined by preincubating sphinganine-N17 with target cells, followed by washing before addition of the virus to initiate infection. We calculated the IC_{50} of the peptide with or without washing the cells (IC_{50} 1 or 2, respectively) to evaluate the ability of residual peptides to sustain inhibitory potency (**Fig. 5*A***). Surprisingly, the IC_{50} value of sphinganine-N17 increased only by 5-fold after cell washing. We compared this with gp41 peptide fusion inhibitors with different membrane-binding properties: C34, which poorly binds membranes, and enfuvirtide, which has an intrinsic membrane-binding ability (41, 42). The IC_{50} of C34 dramatically increased by 305-fold, whereas a 36-fold increase was observed for the IC_{50} of enfuvirtide after cell washing. We then directly treated the viruses with sphinganine-N17, purified the viruses, and added them to the cells. A remarkable reduction in infectivity was observed for the treated viruses (Fig. 5*B*).

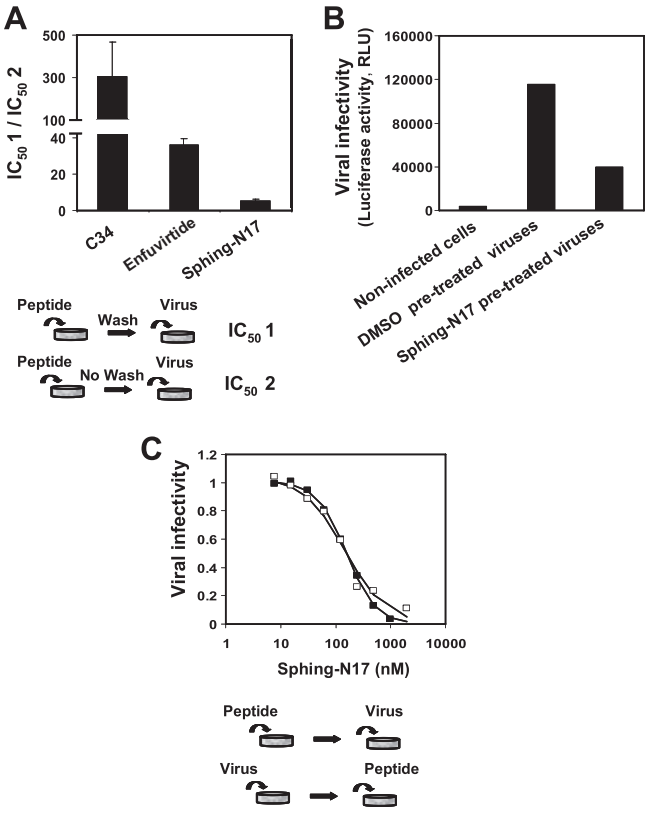

Figure 5. Sphingopeptides strongly bind and accumulate in the cell membrane and in the viral membrane. *A*) Sphingopeptides are strongly anchored to the membrane and sustain a potent inhibitory effect on washing. C34, enfuvirtide, and sphing-N17 were preincubated with TZM-bl cells, followed by washing to remove unbound peptides and the addition of fully infectious viruses to start the infection. IC_{50} of the peptide with or without washing the cells (IC_{50} 1 or 2, respectively) was calculated. Results are presented as the mean ± SD ratio of IC_{50} 1/2 ($n \geq 2$), which reflects the fold increase in IC_{50} after cell washing. *B*) Infectivity of purified viruses that were pretreated with sphing-N17 or DMSO. Infectivity of the purified viruses was measured by luciferase activity in TZM-bl cells and is expressed in relative light units. *C*) Antiviral activity of sphing-N17 when it is preincubated with TZM-bl cells before the addition of fully infectious virus or when it is added to a mixture of the virus with cells.

Furthermore, the sphingopeptides were added to target cells before or after addition of the virus. In the second procedure, both viral and cell membranes are presented at the time of addition, and the sphingopeptides could theoretically bind to any of them. If binding to the viral membrane has a more pronounced effect, we might expect differences in the viral infectivity curves of the compound, depending on the time that the virus was added. Importantly, no difference between the viral infectivity curves was observed for sphinganine-N17 (Fig. 5*C*).

Sphingopeptides preferably bind lipid vesicles enriched in sphingomyelin and cholesterol

The degree of compound association with lipid vesicles was estimated by titrating NBD-labeled compound with

LUVs. The membrane-binding K_a values derived from Eq. 2 are presented in **Table 2**. The data include sphinganine-N17, C16-N17, and enfuvirtide associated with vesicles enriched in sphingomyelin and cholesterol and with vesicles comprising only phosphatidylcholine and cholesterol. The backbone of both palmitic acid and sphinganine is based on a linear saturated carbon chain, and the lipids exhibited similar hydrophobicity. However, palmitic acid-conjugated peptides showed no antiviral activity (Table 1). Thus, the fatty acid conjugates were used as controls for the binding assay of sphingopeptides. Sphinganine-N17 and C16-N17 had higher binding affinities to both types of lipids compared with enfuvirtide. Interestingly, sphinganine-N17 preferably binds lipid vesicles enriched in sphingomyelin and cholesterol (Table 2). Enfuvirtide also exhibits some preference toward these vesicles but to a lesser extent, and C16-N17 retains binding affinity similar to that of both types of vesicles. These observations will be further discussed in the context of the plausible antiviral mode of action of sphingopeptides.

DISCUSSION

The structural organization of lipids in the membrane is a key factor in cell physiology and is exploited by pathogens to infect cells (12). HIV is believed to take advantage of cell membrane-ordered domains to facilitate its entry and budding. These were mainly explored by cholesterol depletion from viral and host cell membranes, together with altering the cellular sphingolipid metabolism before virus-cell fusion (43–48). Much less, however, is known about the recruitment of specific lipid moieties to the site of fusion during the dynamic HIV fusion reaction. A substantial enrichment of dihydrosphingomyelin was observed in HIV particles that bud from their host cells (10). Thus, we hypothesized that its dihydrosphingosine (sphinganine) backbone may penetrate into the site of membrane fusion mediated by the HIV Env. To investigate this, we conjugated sphinganine as well as other lipids to short, otherwise inert, peptides from the HIV-1 Env core and their antiviral activities were investigated in several types of HIV-1 infection assays. The only lipid moiety that endowed potent antiviral activity to the peptides was sphinganine (a summary of the inhibitory IC_{50} is presented in Supplemental Table S1).

The analysis of the interplay between the lipid backbone and its conjugated HIV-1 peptide revealed that the anti-HIV effect is determined both by a specific peptide sequence and by a specific lipid moiety (*i.e.,* sphinganine). This is based on the following findings: first, sphingopeptides exhibited antiviral activity against HIV-1 and not against VSV-G (Fig. 3*A*). Second, mutagenesis analysis of the peptide interactions by knocking out their ability to self-assemble or by randomizing the sequence completely abrogated the antiviral activity of sphingopeptides (Fig. 3*B–D*). Third, sphinganine alone did not alter HIV-1 infection at a concentration at which sphinganine-N17 completely blocked infection (Fig. 4*B*), and fourth, changing the sequence of the peptide, while keeping the same lipid backbone yielded different inhibitory levels (Fig. 4*B, D*).

The viral membrane has a different lipid composition than does the cell membrane (10). This parameter may affect the types of lipids that are bound to the cell and the viral membranes during fusion. We showed that sphingopeptides could inhibit when bound to the cell membrane or to the viral membrane by their fusion inhibitory activity on cell-cell fusion assay; the ability of sphinganine to preserve sufficient amounts of bound peptides within the target cells after washing, which prolonged their antiviral potencies; and the reduced infectivity of viruses pretreated with sphingopeptides.

Membrane binding affinity analysis revealed that sphinganine-N17 preferably binds lipid vesicles enriched in sphingomyelin and cholesterol (Table 2). Several lines of evidence support the interaction of dihydrosphingomyelin with membrane-ordered domains. In model membranes, cholesterol interacts with dihydrosphingomyelin to form more condensed domains than the ones formed with sphingomyelin (49). Studies in bilayers that resemble the ocular lens membranes show that the amount of cholesterol crystallite formation is much higher with dihydrosphingomyelin than with sphingomyelin (50). In addition, the polar dihydrosphingosine base could favor its interaction with the sphingolipid backbone chains through hydrogen bonds (27).

Sphingolipids play an auxiliary function in HIV entry by several proposed models (44). Sphingolipids may

TABLE 2. *Sphinganine-N17 preferably binds lipid vesicles enriched in sphingomyelin and cholesterol*

	K_a (M^{-1})	
Compound	PC:SM:Chol (1:1:1)	PC:Chol (9:1)
Sphinganine-N17	$4.7 \times 10^5 \pm 1 \times 10^5$	$8.4 \times 10^4 \pm 1.4 \times 10^4$
C16-N17	$1.7 \times 10^5 \pm 0.3 \times 10^5$	$1.5 \times 10^5 \pm 0.7 \times 10^5$
Enfuvirtide	$6.4 \times 10^4 \pm 1.4 \times 10^4$	$3.1 \times 10^4 \pm 0.5 \times 10^4$

Compound association with lipid vesicles was estimated by titration of NBD-labeled compound with large unilamellar vesicles. Mole ratio between phosphatidylcholine (PC), sphingomyelin (SM), and cholesterol (Chol) is shown for each vesicle. Membrane-binding constants (K_a) were calculated from Eq. 2 in Materials and Methods. Results represent means ± SD of the fitting curve; $n = 3$.

enhance virus attachment by direct interaction with the HIV-1 envelope (6, 51). In addition, they are involved in clustering of sufficient receptors to the fusion site (52, 53). In intestinal epithelial cells, both gp120 and gp41 bind to galactosyl ceramide, located in membrane-ordered domains. Thus, they allow the transcytosis of the virus across the epithelial barrier (54).

Resistant strains emerge from treatment with gp41 C-peptide fusion inhibitors. Mutations in a contiguous 3-aa sequence within the NHR region, GIV, are often related to the acquisition of viral resistance to enfuvirtide (40). The alterations in that specific region were also observed during phase I of the clinical trial with enfuvirtide (55). We show that sphinganine endows antiviral activities to short conserved N peptides to overcome enfuvirtide-resistant viruses. Hence, there may be implications for the use of derivatives of N peptides as potential microbicides. Possible future applications for sphingopeptides are to extend the half-life time of fusion inhibitors *in vivo* and to act as topical blockers of viral transmission during sexual intercourse.

In summary, the data suggest that sphingopeptides are recruited to the HIV membrane fusion site with enhanced membrane-binding affinity that prolonged their inhibitory potencies. The anti-HIV activity is determined by both the peptides and their sphinganine conjugate. This unique characteristic makes sphingopeptides the shortest lipid-based HIV peptides that potently inhibit viral fusion. Because sphingolipids are involved in many cellular processes such as signaling, viral infection, and membrane trafficking, the present data suggest a general concept of developing inhibitors to sphingolipid-mediated biological systems. FJ

The authors thank Batya Zarmi for her valuable help with peptide purification and Winfried Weissenhorn for providing the recent 3-dimensional structure of gp41. This study was supported by the Israel Science Foundation (to Y.S.) and in part by federal funds (to R.B.) from the Frederick National Laboratory, National Cancer Institute, U.S. National Institutes of Health (contract HHSN26120080001E). The content of this publication does not necessarily reflect the views or policies of the U.S. Department of Health and Human Services, nor does mention of trade names, commercial products, or organizations imply endorsement by the U.S. government. Y.S. is the incumbent of the Harold S. and Harriet B. Brady Professorial Chair in Cancer Research.

REFERENCES

1. White, J. M. (1990) Viral and cellular membrane fusion proteins. *Annu. Rev. Physiol.* **52,** 675–697
2. Chernomordik, L. V., and Kozlov, M. M. (2008) Mechanics of membrane fusion. *Nat. Struct. Mol. Biol.* **15,** 675–683
3. Nguyen, D. H., and Hildreth, J. E. (2000) Evidence for budding of human immunodeficiency virus type 1 selectively from glycolipid-enriched membrane lipid rafts. *J. Virol.* **74,** 3264–3272
4. Ono, A., and Freed, E. O. (2001) Plasma membrane rafts play a critical role in HIV-1 assembly and release. *Proc. Natl. Acad. Sci. U. S. A.* **98,** 13925–13930
5. Viard, M., Parolini, I., Sargiacomo, M., Fecchi, K., Ramoni, C., Ablan, S., Ruscetti, F. W., Wang, J. M., and Blumenthal, R. (2002) Role of cholesterol in human immunodeficiency virus type 1 envelope protein-mediated fusion with host cells. *J. Virol.* **76,** 11584–11595
6. Mahfoud, R., Garmy, N., Maresca, M., Yahi, N., Puigserver, A., and Fantini, J. (2002) Identification of a common sphingolipid-binding domain in Alzheimer, prion, and HIV-1 proteins. *J. Biol. Chem.* **277,** 11292–11296
7. Takeda, M., Leser, G. P., Russell, C. J., and Lamb, R. A. (2003) Influenza virus hemagglutinin concentrates in lipid raft microdomains for efficient viral fusion. *Proc. Natl. Acad. Sci. U. S. A.* **100,** 14610–14617
8. Choi, K. S., Aizaki, H., and Lai, M. M. (2005) Murine coronavirus requires lipid rafts for virus entry and cell-cell fusion but not for virus release. *J. Virol.* **79,** 9862–9871
9. Medigeshi, G. R., Hirsch, A. J., Streblow, D. N., Nikolich-Zugich, J., and Nelson, J. A. (2008) West Nile virus entry requires cholesterol-rich membrane microdomains and is independent of αvβ3 integrin. *J. Virol.* **82,** 5212–5219
10. Brugger, B., Glass, B., Haberkant, P., Leibrecht, I., Wieland, F. T., and Krausslich, H. G. (2006) The HIV lipidome: a raft with an unusual composition. *Proc. Natl. Acad. Sci. U. S. A.* **103,** 2641–2646
11. Simons, K., and Ikonen, E. (1997) Functional rafts in cell membranes. *Nature* **387,** 569–572
12. Simons, K., and Gerl, M. J. (2010) Revitalizing membrane rafts: new tools and insights. *Nat. Rev. Mol. Cell Biol.* **11,** 688–699
13. Berger, E. A., Murphy, P. M., and Farber, J. M. (1999) Chemokine receptors as HIV-1 coreceptors: roles in viral entry, tropism, and disease. *Annu. Rev. Immunol.* **17,** 657–700
14. Eckert, D. M., and Kim, P. S. (2001) Mechanisms of viral membrane fusion and its inhibition. *Annu. Rev. Biochem.* **70,** 777–810
15. Gallo, S. A., Finnegan, C. M., Viard, M., Raviv, Y., Dimitrov, A., Rawat, S. S., Puri, A., Durell, S., and Blumenthal, R. (2003) The HIV Env-mediated fusion reaction. *Biochim. Biophys. Acta* **1614,** 36–50
16. Chien, M. P., Jiang, S., and Chang, D. K. (2008) The function of coreceptor as a basis for the kinetic dissection of HIV type 1 envelope protein-mediated cell fusion. *FASEB J.* **22,** 1179–1192
17. Finzi, A., Xiang, S. H., Pacheco, B., Wang, L., Haight, J., Kassa, A., Danek, B., Pancera, M., Kwong, P. D., and Sodroski, J. (2010) Topological layers in the HIV-1 gp120 inner domain regulate gp41 interaction and CD4-triggered conformational transitions. *Mol. Cell* **37,** 656–667
18. Jiang, S., Lin, K., Strick, N., and Neurath, A. R. (1993) HIV-1 inhibition by a peptide. *Nature* **365,** 113
19. Furuta, R. A., Wild, C. T., Weng, Y., and Weiss, C. D. (1998) Capture of an early fusion-active conformation of HIV-1 gp41. *Nat. Struct. Biol.* **5,** 276–279
20. Chan, D. C., and Kim, P. S. (1998) HIV entry and its inhibition. *Cell* **93,** 681–684
21. Melikyan, G. B., Egelhofer, M., and von Laer, D. (2006) Membrane-anchored inhibitory peptides capture human immunodeficiency virus type 1 gp41 conformations that engage the target membrane prior to fusion. *J. Virol.* **80,** 3249–3258
22. Munoz-Barroso, I., Durell, S., Sakaguchi, K., Appella, E., and Blumenthal, R. (1998) Dilation of the human immunodeficiency virus-1 envelope glycoprotein fusion pore revealed by the inhibitory action of a synthetic peptide from gp41. *J. Cell Biol.* **140,** 315–323
23. Colman, P. M., and Lawrence, M. C. (2003) The structural biology of type I viral membrane fusion. *Nat. Rev. Mol. Cell Biol.* **4,** 309–319
24. Chan, D. C., Fass, D., Berger, J. M., and Kim, P. S. (1997) Core structure of gp41 from the HIV envelope glycoprotein. *Cell* **89,** 263–273
25. Weissenhorn, W., Dessen, A., Harrison, S. C., Skehel, J. J., and Wiley, D. C. (1997) Atomic structure of the ectodomain from HIV-1 gp41. *Nature* **387,** 426–430
26. Sollner, T. H. (2004) Intracellular and viral membrane fusion: a uniting mechanism. *Curr. Opin. Cell Biol.* **16,** 429–435
27. Goni, F. M., and Alonso, A. (2006) Biophysics of sphingolipids I. Membrane properties of sphingosine, ceramides and other simple sphingolipids. *Biochim. Biophys. Acta* **1758,** 1902–1921
28. Futerman, A. H., and Riezman, H. (2005) The ins and outs of sphingolipid synthesis. *Trends Cell Biol.* **15,** 312–318

29. Merrifield, R. B., Vizioli, L. D., and Boman, H. G. (1982) Synthesis of the antibacterial peptide cecropin A (1-33). *Biochemistry* **21,** 5020–5031
30. Wexler-Cohen, Y., Ashkenazi, A., Viard, M., Blumenthal, R., and Shai, Y. (2010) Virus-cell and cell-cell fusion mediated by the HIV-1 envelope glycoprotein is inhibited by short gp41 N-terminal membrane-anchored peptides lacking the critical pocket domain. *FASEB J.* **24,** 4196–4202
31. Garg, H., Joshi, A., Freed, E. O., and Blumenthal, R. (2007) Site-specific mutations in HIV-1 gp41 reveal a correlation between HIV-1-mediated bystander apoptosis and fusion/hemifusion. *J. Biol. Chem.* **282,** 16899–16906
32. Lev, N., and Shai, Y. (2007) Fatty acids can substitute the HIV fusion peptide in lipid merging and fusion: an analogy between viral and palmitoylated eukaryotic fusion proteins. *J. Mol. Biol.* **374,** 220–230
33. Hetru, C., Letellier, L., Oren, Z., Hoffmann, J. A., and Shai, Y. (2000) Androctonin, a hydrophilic disulphide-bridged non-haemolytic anti-microbial peptide: a plausible mode of action. *Biochem. J.* **345**(Pt. 3), 653–664
34. Ben-Efraim, I., Bach, D., and Shai, Y. (1993) Spectroscopic and functional characterization of the putative transmembrane segment of the minK potassium channel. *Biochemistry* **32,** 2371–2377
35. Holguin, A., De Arellano, E. R., and Soriano, V. (2007) Amino acid conservation in the gp41 transmembrane protein and natural polymorphisms associated with enfuvirtide resistance across HIV-1 variants. *AIDS Res. Hum. Retroviruses* **23,** 1067–1074
36. Chan, D. C., Chutkowski, C. T., and Kim, P. S. (1998) Evidence that a prominent cavity in the coiled coil of HIV type 1 gp41 is an attractive drug target. *Proc. Natl. Acad. Sci. U. S. A.* **95,** 15613–15617
37. Wexler-Cohen, Y., and Shai, Y. (2009) Membrane-anchored HIV-1 N-heptad repeat peptides are highly potent cell fusion inhibitors via an altered mode of action. *PLoS Pathog.* **5,** e1000509
38. Eckert, D. M., and Kim, P. S. (2001) Design of potent inhibitors of HIV-1 entry from the gp41 N-peptide region. *Proc. Natl. Acad. Sci. U. S. A.* **98,** 11187–11192
39. Bewley, C. A., Louis, J. M., Ghirlando, R., and Clore, G. M. (2002) Design of a novel peptide inhibitor of HIV fusion that disrupts the internal trimeric coiled-coil of gp41. *J. Biol. Chem.* **277,** 14238–14245
40. Baldwin, C. E., Sanders, R. W., Deng, Y., Jurriaans, S., Lange, J. M., Lu, M., and Berkhout, B. (2004) Emergence of a drug-dependent human immunodeficiency virus type 1 variant during therapy with the T20 fusion inhibitor. *J. Virol.* **78,** 12428–12437
41. Wexler-Cohen, Y., and Shai, Y. (2007) Demonstrating the C-terminal boundary of the HIV 1 fusion conformation in a dynamic ongoing fusion process and implication for fusion inhibition. *FASEB J.* **21,** 3677–3684
42. Liu, S., Lu, H., Niu, J., Xu, Y., Wu, S., and Jiang, S. (2005) Different from the HIV fusion inhibitor C34, the anti-HIV drug Fuzeon (T-20) inhibits HIV-1 entry by targeting multiple sites in gp41 and gp120. *J. Biol. Chem.* **280,** 11259–11273
43. Liao, Z., Cimakasky, L. M., Hampton, R., Nguyen, D. H., and Hildreth, J. E. (2001) Lipid rafts and HIV pathogenesis: host membrane cholesterol is required for infection by HIV type 1. *AIDS Res. Hum. Retroviruses* **17,** 1009–1019
44. Rawat, S. S., Johnson, B. T., and Puri, A. (2005) Sphingolipids: modulators of HIV-1 infection and pathogenesis. *Biosci. Rep.* **25,** 329–343
45. Ablan, S., Rawat, S. S., Viard, M., Wang, J. M., Puri, A., and Blumenthal, R. (2006) The role of cholesterol and sphingolipids in chemokine receptor function and HIV-1 envelope glycoprotein-mediated fusion. *Virol. J.* **3,** 104
46. Viard, M., Parolini, I., Rawat, S. S., Fecchi, K., Sargiacomo, M., Puri, A., and Blumenthal, R. (2004) The role of glycosphingolipids in HIV signaling, entry and pathogenesis. *Glycoconj. J.* **20,** 213–222
47. Finnegan, C. M., Rawat, S. S., Puri, A., Wang, J. M., Ruscetti, F. W., and Blumenthal, R. (2004) Ceramide, a target for antiretroviral therapy. *Proc. Natl. Acad. Sci. U. S. A.* **101,** 15452–15457
48. Vieira, C. R., Munoz-Olaya, J. M., Sot, J., Jimenez-Baranda, S., Izquierdo-Useros, N., Abad, J. L., Apellaniz, B., Delgado, R., Martinez-Picado, J., Alonso, A., Casas, J., Nieva, J. L., Fabrias, G., Manes, S., and Goni, F. M. (2010) Dihydrosphingomyelin impairs HIV-1 infection by rigidifying liquid-ordered membrane domains. *Chem. Biol.* **17,** 766–775
49. Kuikka, M., Ramstedt, B., Ohvo-Rekila, H., Tuuf, J., and Slotte, J. P. (2001) Membrane properties of D-erythro-N-acyl sphingomyelins and their corresponding dihydro species. *Biophys. J.* **80,** 2327–2337
50. Epand, R. M. (2003) Cholesterol in bilayers of sphingomyelin or dihydrosphingomyelin at concentrations found in ocular lens membranes. *Biophys. J.* **84,** 3102–3110
51. Hammache, D., Pieroni, G., Yahi, N., Delezay, O., Koch, N., Lafont, H., Tamalet, C., and Fantini, J. (1998) Specific interaction of HIV-1 and HIV-2 surface envelope glycoproteins with monolayers of galactosylceramide and ganglioside GM3. *J. Biol. Chem.* **273,** 7967–7971
52. Finnegan, C. M., Rawat, S. S., Cho, E. H., Guiffre, D. L., Lockett, S., Merrill, A. H., Jr., and Blumenthal, R. (2007) Sphingomyelinase restricts the lateral diffusion of CD4 and inhibits human immunodeficiency virus fusion. *J. Virol.* **81,** 5294–5304
53. Rawat, S. S., Viard, M., Gallo, S. A., Blumenthal, R., and Puri, A. (2006) Sphingolipids, cholesterol, and HIV-1: a paradigm in viral fusion. *Glycoconj. J.* **23,** 189–197
54. Alfsen, A., Iniguez, P., Bouguyon, E., and Bomsel, M. (2001) Secretory IgA specific for a conserved epitope on gp41 envelope glycoprotein inhibits epithelial transcytosis of HIV-1. *J. Immunol.* **166,** 6257–6265
55. Wei, X., Decker, J. M., Liu, H., Zhang, Z., Arani, R. B., Kilby, J. M., Saag, M. S., Wu, X., Shaw, G. M., and Kappes, J. C. (2002) Emergence of resistant human immunodeficiency virus type 1 in patients receiving fusion inhibitor (T-20) monotherapy. *Antimicrob. Agents Chemother.* **46,** 1896–1905
56. Buzon, V., Natrajan, G., Schibli, D., Campelo, F., Kozlov, M. M., and Weissenhorn, W. (2010) Crystal structure of HIV-1 gp41 including both fusion peptide and membrane proximal external regions. *PLoS Pathog.* **6,** e1000880

Received for publication June 13, 2012.
Accepted for publication July 24, 2012.